ISSN No: -2456-2165 https://doi.org/10.38124/ijisrt/25oct1379

Artificial Intelligence and Machine Learning Driven Multiplex Programmable Modelling for Refractive Index Based Surface Plasmon Resonance Sensor

Shalini Srivastava[1]; Shambhavi Mudra Shukla[1]; Nishant Singh[1]; Parimal Tiwari[1]; Ramesh Mishra[1]; Vaibhava Srivastava[2]; Mukesh Mishra[3]; Sachin Singh[3]; Vipin Sharma[4]

[1]Department of Electronics & Communication Engineering Institute of Engineering & Technology Dr. Ram Manohar Lohia Avadh University, Ayodhya (U.P.), India
[2]Department of Electrical and Electronics Engineering, Shri Ramswaroop Memorial University, Lucknow- Deva Road, Barabanki, Uttar Pradesh, India
[3]Faculty of Physical Sciences, Shri Ramswaroop Memorial University, Lucknow-Deva Road, Barabanki, Uttar Pradesh, India
[4]Department of Physics Rana Pratap Post Graduate College, Sultanpur

Publication Date: 2025/11/06

Abstract: Researchers can employ various optical biosensor technologies in many biomedical diagnostic and analysis procedures because they can assess the conformational changes of biomolecules and their molecular interactions. Surface plasmon resonance biosensors are one of the most popular methods among many optical biosensors because they are utilized for label-free and real-time monitoring with outstanding precision and accuracy. The current study proposes AI and machine learning (ML) programming-based rapid and highly sensitive SPR refractive sensor. The proposed SPR biosensor device consists of a glass prism N-FK51A, silver metal, graphene, nickel, and potassium niobate layers. Attenuated total reflection (ATR) is the basis for the device operation, and the Kretschmann configuration serves as the foundation for the device structure. The performance parameters, such as angular sensitivity, quality factor, detection accuracy, limit of detection and electric filed have been numerically analysed for blood sample. It is possible to identify and examine biomolecules with the proposed surface plasmon resonance biosensor.

Keywords: *Artificial Intelligence, Machine Learning, Programmable, Algorithms, Optical Sensor.*

How to Cite: Shalini Srivastava; Shambhavi Mudra Shukla; Nishant Singh; Parimal Tiwari; Ramesh Mishra; Vaibhava Srivastava; Mukesh Mishra; Sachin Singh; Vipin Sharma (2025). Artificial Intelligence and Machine Learning Driven Multiplex Programmable Modelling for Refractive Index Based Surface Plasmon Resonance Sensor. *International Journal of Innovative Scienceand Research Technology*,10(10), 2551-2563. https://doi.org/10.38124/ijisrt/25oct1379

I. INTRODUCTION

The rapid advancement in artificial intelligence (AI) and machine learning (ML) has given rise to neural networks, pattern recognition, cognitive computing, and robotics which play a crucial role in facilitating complex model analysis.AI is engaged in collaborative efforts across various domains, leveraging machine learning methodologies. An AI-driven application facilitates system improvement, knowledge, and complex programming while necessitating minimal human resources, flexibility, accuracy, and sustainable viability [1]. Recently, applying real-time AI models for data analysis, aimed at furnishing decision support capabilities for complex datasets [2]. The models for AI systems are developed in consideration ofhuman behavior, especially, in the realm of exhibiting human-like cognitive thinking and reasoning abilities [3]. These models extract information from databases and convert them into actionable knowledge. The transformative process is accomplished with a set of pre-defined algorithms usingML [4-5].

The set of ML algorithms defined for AI models to process the transformative task in real-time has gained a signified interest in recent years. Notably, the ML model is

ISSN No: -2456-2165 https://doi.org/10.38124/ijisrt/25oct1379

the fundamental unit in the spectroscopy technique incorporating emission spectra focused on the material surface to swiftly produce outcomes for diverse samples without necessitating intricate pre-processing procedures [4]. The AI and ML integrated systemshave tremendous advancements in various fields such as robotics, healthcare, and computer vision [6-8].These integrated systems possess the capability to identify relevant patterns within a vast amount of information, thereby addressing an unmet need. The systems differ from traditional statistical methods prioritizing prediction and classification based on high-dimensional data rather than inference [9]. Artificial neural networks, drawing inspiration from the intricate architecture of the human brain, have emerged as a preeminent machine learning technique [10-12]. This network tackles intricate inverse quandaries concerning the design of functional nanostructure, advancing the field of ML microscopy and imaging, discerning quantum states, and pioneering all-optical machine learning, all while maintaining remarkable accuracy and temporal efficiency [11-15].

The establishment of a learning health system, characterized by a continuous cycle of systematically gathering and analyzing health data to derive novel insights that inform healthcare decisions and drive system enhancements, is a paramount global priority [16-18].The application of AI and ML in healthcare enables the stratification of patients based on large data, which holds implications for various aspects of their care, including risk estimation for autoimmune diseases, diagnosis, initial and ongoing management, monitoring, treatment response, and outcome assessment [19-20].Traditional statistical models focus on uncovering relationships and confidence intervals between data points and outcomes. In contrast, ML methods prioritize achieving high prediction accuracy, with less emphasis on interpretability.

The imminent future holds the anticipation of a medical revolution fueled by advancements in AI. ML-based individualized prediction has the potential to revolutionize complex medical scenarios, including fields such as nephrology, cardiology, and ophthalmology [21-25]. Additionally, intelligent telehealth computing has demonstrated significant promise in facilitating cost-effective applications of medical AI. However, despite the broad scope of these technologies, the complete integration of prediction and telehealth has yet to be accomplished, and the actual benefits of AI in terms of healthcare quality and socioeconomic impact are still to be validated [26-30]. The convergence of quantum computing and artificial intelligence holds immense potential to reshape the landscape of future technologies, ushering in a profound era of transformation. The rapid advancement in ML algorithms has gained significant momentum to cater to the diverse requirements of big data applications. Among these algorithms, programmable classifiers play a crucial role by effectively processing both discrete and continuous input features to generate binary predictions or outcomes. These predictions aim to closely align with binary targets, such as determining the presence or absence of a disease or predicting the success or failure of a device [31-34].

Due to the exponential expansion in model size, coupled with the corresponding rise in computational intricacy and rapid surge in data volume, the development of precise AI/ML models faces critical challenges regarding sustainability in energy, storage, computing power, networking, and domain expertise. In healthcare applications benefiting from robust computing infrastructure, the energy consumption associated with operating large-scale AI/ML models also encounters sustainability problems arising from the deceleration in hardware platform advancements. As model sizes increase, the amount of health data necessary for training grows dramatically. For healthcare applications relying on network connections to access cloud servers, the upgrading and maintenance of current storage infrastructures pose storage sustainability concerns, accompanied by exorbitant costs. Furthermore, applications restricted to edge computation on embedded hardware confront even more severe sustainability issues in energy, computing power, networking, and storage due to existing limitations in power, as well as areas like security, privacy, and latency. Aside from sustainability problems linked to hardware, the scarcity of domain expertise in health data labeling has impeded the progress of AI/ML in healthcare. While attempts have been made to address specific resource constraints in AI/ML for healthcare, the proposed methods have primarily focused on the development of a multilayer programmable AI model for multiplex expressions for simultaneous analysis [35-38]. Insufficient methods are available for the interpretation of the clinical and ‘omic data. AI and ML techniques are capable to study the patterns from the abundance of information with the achievement of the challenges faced. The classification of patients based on the data has outcomes for their diagnostic procedure, treatment, monitoring, and management [39-40].

Optical biosensors have applications in various fields like agriculture, biomedical, and environmental monitoring. Optoelectricnanosensors can determine the molecular and biological orientations promoting their integration into biomedical diagnosis and analysis. Based on mechanism and molecules several classifications of Nano-Biosensors have been already reported among this array of available platforms surface plasmon resonance (SPR)-based Nano-Biosensors employ plasmonic principles, exhibiting exceptional precision and accuracy. The data obtained from the sensors are applied to different ML models for diagnosis and prognosis. This proposed study describes an innovative AI model based on ML for cancer detection by utilizing reflective light angles on the material surface. The SPR-based optical biosensor has various advantages such as precise binding affinity, high throughput, and economical [41-42]. Presently ML models have been reported for the prediction of diseases such as mental health, cancer, diabetes, autism, COVID-19 and multiple sclerosis. An ML model has been reported by Vitor and Clebera to determine the period of patients allowed to stay in specialized care facilities when suffering from COVID-19 this model operates on physiological parameters. Although the available studies are based on the physical and physiological parameters obtained from the biosensors limited work has been carried out for the development of highly specific and accurate biosensors [43]. For this current study we first explore the datasets determined

ISSN No: -2456-2165 https://doi.org/10.38124/ijisrt/25oct1379

with the SPR-sensing for cancer detection and classification, this study can facilitate the advancement of upcoming highly accurate, and specific biomedical device development. The reflective angles on the surface of the material are determined and the parameters are used for the classification and analysis. Although the generation of reflective angles for diverse surfaces and biomolecules deposition entails considerable labor and expense, the present study establishes a foundational framework for the development of ML-based models tailored to SPR-based Nano-Biosensors. These models enable comprehensive testing and prediction of biosensor performance across diverse parameter regimes.

This presented model is based on AI and ML-driven methodology [44-45]. The implementation of AI technology will catalyze the substantial quantification and progress of the model. Thebimetallic materials (silver, graphene, nickel, and Potassium niobate) provide a synergistic effect on the system. The incorporation of silver nanoparticles is anticipated to enhance the sensitivity of the surface plasmon resonance model. In this approach, the introduction of colloidal silver nanoparticles influences the attenuated total reflection curves by causing a shift in the angle of SPR reflectance, thereby elongating the curve and resulting in an augmentation of the minimum reflectivity. The current algorithm for proposed SPR sensor has been developed by MATLAB 2019a software. In the current study AI/ML based SPR sensor leverage machine learning techniques have been used to enhance the performance and accuracy of SPR sensors. This SPR sensor detect the change in refractive index shifts caused by bimolecular interactions. The multilayer AI and ML based SPR sensor further utilizes programmable logic gates as its foundation. Itemployesa binary encoding scheme with inputs “00, 01, 10, 11”. The data recorded were further analyzed using an AI-based artificial neural network (ANN) machine learning algorithm.

II. MODELLING AND SIMULATION STUDY

➢ *Theoratical Modelling*

The Kretschmann configuration is used for the suggested sensor structure. The angular interrogation approach, in which the wavelength at 633 nm remains constant but the incidence angle varies, is used to numerically carried out the proposed task. This SPR sensor consists five layers such as silver (Ag) metal, graphene (G), Nickel (Ni), Potassium Niobate ($KNbO_3$), and the N-KF51A Prism. An optical source is used to incident light on the prism with a wavelength of 633 nm, and the other side of the coupling prism is used to measure the refracted light concurrently. The attenuation of reflected light is measured using a detector and computer system. This work uses the N-KF51A prism as a coupling medium. The low refractive index of the N-KF51A prism is useful for effectively removing angular error during setup. As seen in Fig. 1(A), the glass with a lower RI significantly shifts the reflectance curve and causes severe angular sensitivity when viewed through a different prism for the proposed biosensor. Figure 1(A) shows the suggested SPR biosensor construction while the Fig.1(B) shows the possible sequential experimental procedure for their deposition.

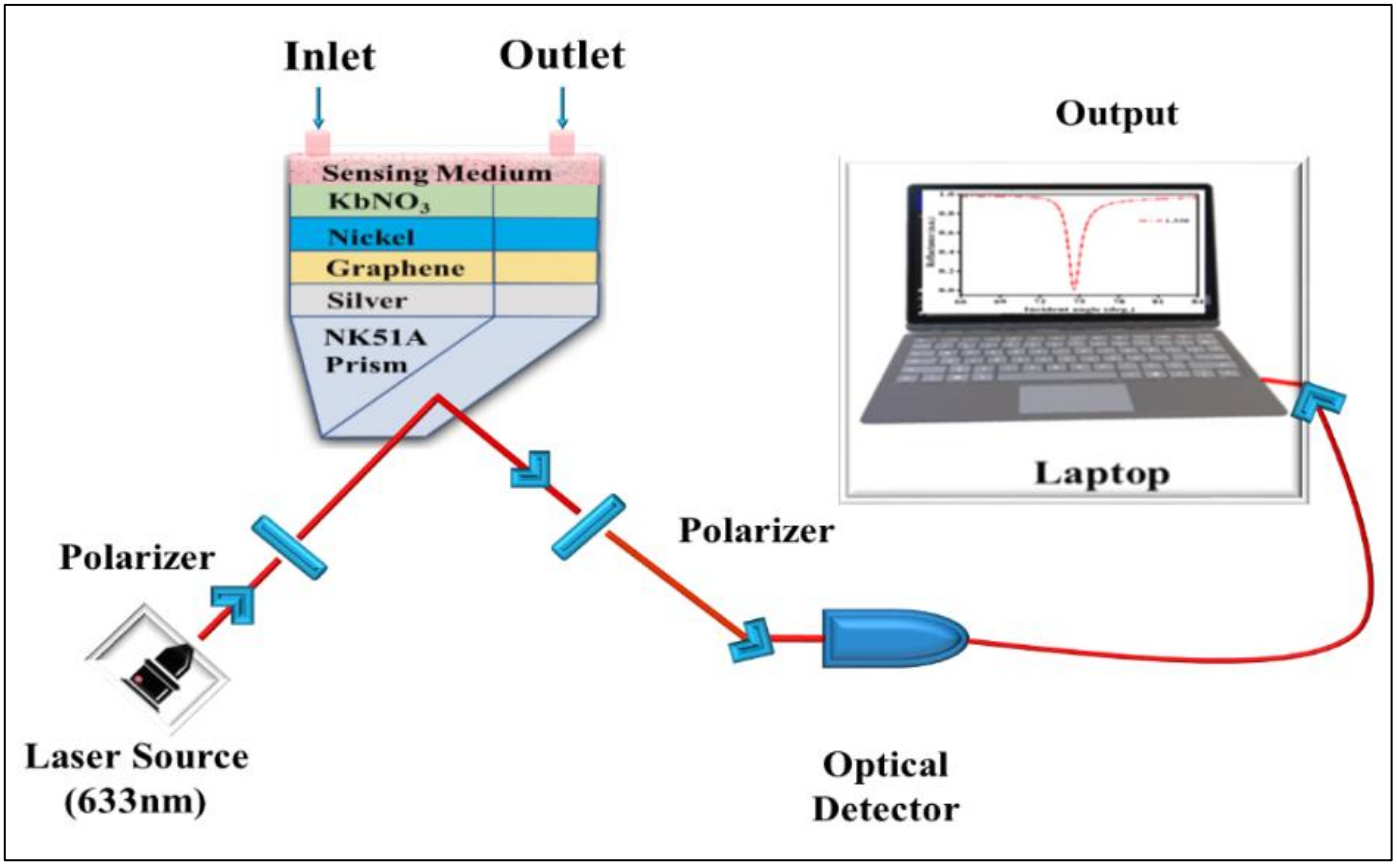

Fig 1 (A) Proposed Multilayer Structure of Surface Plasmon Resonance Sensor.

ISSN No: -2456-2165 https://doi.org/10.38124/ijisrt/25oct1379

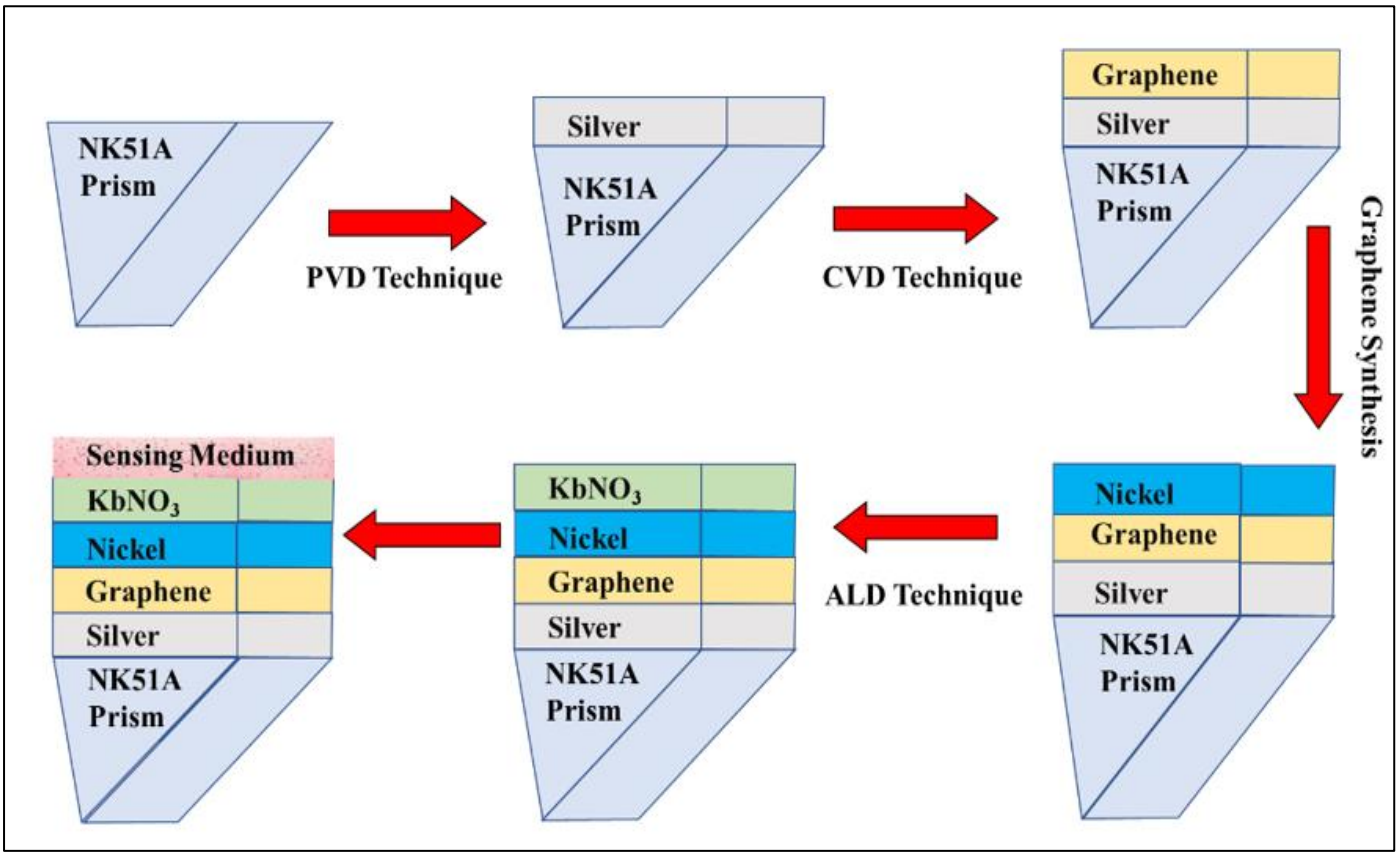

Fig 1(B) Experimental Procedure of Multilayer Deposition Techniques Using for Proposed Surface Plasmon Resonance Sensor.

Table 1 Design Parameters of Used Materials for Proposed SPR Biosensor at 633nm Wavelength.

Materials	Thickness (nm)	Refractive index at 633nm
N-KF51A Prism	100.00	1.4853
Silver Metal (Ag)	45.00	0.0562+4.2776*i
Graphene (G)	0.34	3.0+1.40*i
Nickel (Ni)	20.00	0.0319+2.9631*i
Potassium Niobate ($KNbO_3$)	5.00	2.1686

➢ *Mathematical Modelling*

- *Work Methodology*

The development of a multilayer Kretschmann configuration based SPR sensor is envisaged for medical diagnosis in this project proposal. As a first step for pre-experiment simulation work, we need to calculate the RI of each layer at the incident wavelength of monochromatic light. The RI of the glass prism (BK7, CaF_2, SF10, NKF51A etc.) has been calculated with the help of the Sellmeier relation [46].

$$n^2_{NKF51A} = \left(1 + \frac{1.03961212\times\lambda^2}{\lambda^2-0.00600069867} + \frac{0.231792344\times\lambda^2}{\lambda^2-0.0200179144} + \frac{1.001046945\times\lambda^2}{\lambda^2-103.560653}\right) \quad (1)$$

In Eq. (1), λ is the incident wavelength (in μm) of the laser source.

The metal layer deposited on the prism base is required to generate the plasmons at the metal-dielectric interface. For the metal layer deposition over the prism surface, the physical vapour deposition (PVD) technique can be used. The silver metal complex dielectric constant has been calculated by Lorentz- Drude formla and it is defined as the following equation [47]:

$$E_{Ag} = 1 - \left[\frac{\lambda^2\lambda_C}{\lambda_P^2\ [\lambda_C+i\lambda]}\right] \quad (2)$$

Here, λ_p and λ_c represents the plasma and collision wavelengths respectively. The numerical value of λ_p and λ_c for Ag are 1.4591×10^{-7} m and 1.7614×10^{-5} m respectively and λ = 633 nm is wavelength of incident wavelength of light (He-Ne laser light).

The next layers graphene (G) and Nickel (Ni) are coated over metal surface through chemical vapor deposition (CVD) technique. The thickness of monolayer graphene (G) and Nickel (Ni) are 0.34 and 20 nm respectively. After that, last layer of Potassium Niobate ($KNbO_3$) has been deposited on the top of these multilayers. The monochromatic sorce of light incident through prism surface then surface plasmon

ISSN No: -2456-2165 https://doi.org/10.38124/ijisrt/25oct1379

resonance sensing phenomena takes place. Finally, optimized the sensing curves on the computer screen.

- *Transfer Matrix Method (TMM)*

The condition of resonance will be satisfied when the propagation constant of incoming photons matches with the propagation constant of SPs wave. In the resonance condition, the following equation must satisfy [48]:

$$k_x = \left(\frac{2\pi}{\lambda}\right) n_p \sin\theta_i = k_{spw} \quad (3)$$

Where k_x is the horizontal component of propagation constant of incident light, λ is wavelength of incident light, n_p is refractive index of prism and θ_i is incident angle of light and k_{spw} is propagation constant of surface plasmon. First, the transverse magnetic (TM) or p-polarized light should be incident and second that the propagation constant of incident light must match with the surface plasmon are the two necessary conditions for the surface plasmon resonance [49].

When the complete energy of photons is transferred to surface plasmons then a sharp dip has been obtained then the SPR curve reflectance is plotted against the incident angle of light. The optical sensor properties like reflectance and transmittance of multilayer layer stacked devices can be optimized by three methods. They arethe transfer matrix method, field element method, and resultant wave method. However, the transfer matrix method (TMM) has many advantages among them. TMM gives much more accurate results and does not require any approximation. The present work considers the N-layer model study, transfer matrix approach, and Fresnel equation. The tangential component of the electromagnetic field at the first and last surface boundary follows the relation as given as [50]:

$$[E_1 M_1] = X_{ij}[E_{N-1} M_{N-1}] \quad (4)$$

Where, E_1, E_{N-1} and M_1, M_{N-1}, respectively, stand for the electric and magnetic field components of the first and last surfaces.

For an integrated structure, the characteristics matrix X_{ij} is described as follows:

$$X_{ij} = [X_{11} X_{12} X_{21} X_{22}] = \prod_{K=2}^{N-1} X_k \quad (5)$$

With

$$X_k = \left[\cos\beta_k \frac{-i\sin\beta_k}{q_k} - i q_k \sin\beta_k \cos\beta_k\right] \quad (6)$$

Where X_{11}, X_{12}, X_{21}, and X_{22} represent the transfer matrix elements respectively. k is any arbitrary number and β_k represents the phase thickness and q_k represents the refractive indices of corresponding layers and it is defined as [51]:

$$Q_k = \left[\frac{(\epsilon_k - n_1^2 \sin^2\theta)^{\frac{1}{2}}}{\epsilon_k}\right] \quad (7)$$

$$\beta_k = \left[\frac{2\pi d_k \ (\epsilon_k - n_1^2 \sin^2\theta)^{\frac{1}{2}}}{\lambda}\right] \quad (8)$$

Here n_1, θ and λ stand for the prism's refractive index, incident angle, and incident wavelength, respectively. In addition, d_k and ϵ_k are the k^{th} layer thickness and dielectric constant, respectively. The following formulas can be used to determine the reflectivity (R_P) and reflection coefficient (r) for incident p-polarized light.

$$R_P = |r|^2 = \left[\frac{(X_{11} + X_{12} q_N) q_1 - (X_{21} + X_{22} q_N)}{(X_{11} + X_{12} q_N) q_1 + (X_{21} + X_{22} q_N)}\right] \quad (9)$$

- *Performance Parameters*

The evaluation of the sensing performance of SPR sensors depends on a few key factors. These are Sensitivity (S), Full width at half maxima (FWHM), Figure of merit (FoM), Detection accuracy (DA), and detection limit (LoD).

✓ *Sensitivity (S)*

If the refractive index of the sensing medium changes by Δn, and the resulting shift in the SPR angle is$\Delta\theta_{res}$, then:

$$S = \left[\frac{\Delta\theta_{res}}{\Delta n}\right] \quad (10)$$

✓ *Full Width at Half Maxima (FWHM)*

It measures the width of SPR curve at half of its maximum value. It defines the sharpness of the reflectance curve. It is essential to consider FWHM because it is used to determine the majority of metrics, including DA and FoM. It needs to be described as with a minimum value.

$$FWHM = \frac{1}{2}[(\theta_{max} - \theta_{min})] \quad (11)$$

✓ *Detection Accuracy (DA)*

It is inversely related to the FWHM value. Additionally called the signal-to-noise ratio. It should have the highest possible value:

$$DA = \left[\frac{1}{FWHM}\right] \quad (12)$$

✓ *Figure of Merit (FoM)*

Quality factor (QF) is another name for the figure of merit. It is mathematically calculated using the sensitivity-to-FWHM ratio and is shown as follows:

$$FoM = \left[\frac{S}{FWHM}\right] \quad (13)$$

✓ *Limit of Detection (LoD)*

It measures the smallest fluctuation in the RI of the detecting layer that the suggested sensor can analyse:

$$LoD = \left[\frac{1}{S}\right] \times 0.001° \quad (14)$$

ISSN No: -2456-2165 https://doi.org/10.38124/ijisrt/25oct1379

✓ *Phase Angle and Electric Field Intensity Enhancement Factor (EFIEF)*

At the metal-dielectric interface, the phase angle of p-polarized light is defined as:

$$\Phi = \arg\circledR \tag{15}$$

The ratio of the electric field intensity squared at the sensor layer to first layer interface is known as the electric field intensity enhancement factor (EFIEF). Mathematically it is defined as:

$$\text{EFIEF} = \left|\frac{E\left(\frac{L}{L-1}\right)}{E\left(\frac{1}{2}\right)}\right|^2 = \frac{\varepsilon_1}{\varepsilon_L}\left|\frac{E\left(\frac{L}{L-1}\right)}{E\left(\frac{1}{2}\right)}\right|^2 = \left[\frac{\varepsilon_1}{\varepsilon_L}\right]|t|^2 \tag{16}$$

Where, t is the transmittance, ϵ_1 and ϵ_L are the first and last layer dielectric constants respectively.

- *Machine Learing and Artificial Intelligence Data Set and Pre-Processing Steps*

The study focuses at an artificial intelligence program that would make the simulation process easier for regular users, software called MATLAB 2019a has been utilized. To automatically choose the preferred mode, which is otherwise selected visually by the experts, the algorithm recommends one deep learning model and standard machine learning. It can be incorporated as a module in academic programs or as an add-on into commercial applications. Throughout the entire design process, the suggested innovative step has saved about sixty minutes. Mode selection of optical sensors, such as SPR sensing geometries, can also benefit from the current work. For an overview of the ensuing procedures of machine learning and artificial intelligence in optical sensors, a block diagram has been provided in Fig. 2.

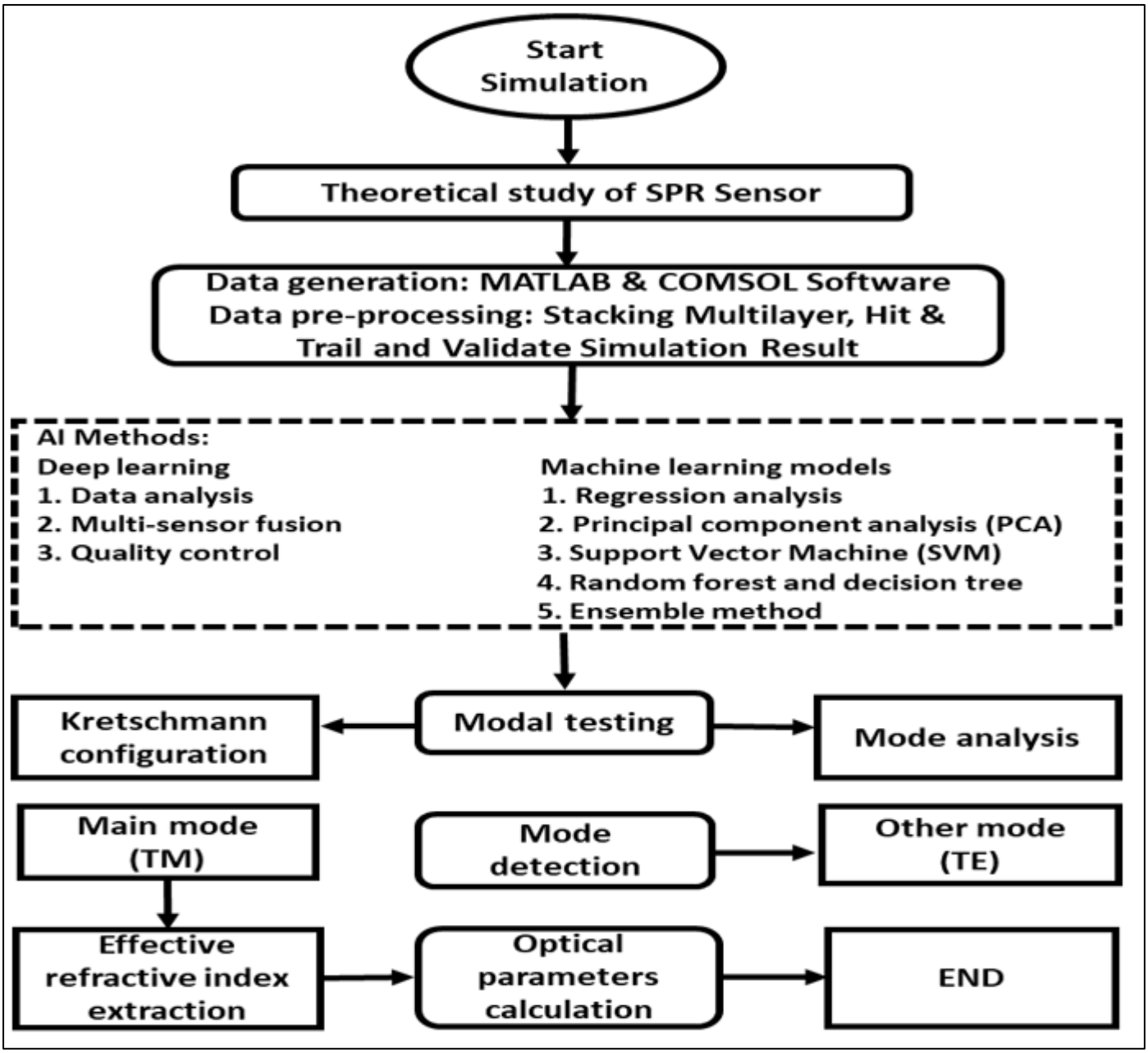

Fig 2 Block Diagram of AI and ML Steps.

ISSN No: -2456-2165 https://doi.org/10.38124/ijisrt/25oct1379

III. RESULT AND DISCUSSION

➢ *Evaluation of Different SPR Models*

In this section, many surface plasmon resonance (SPR) sensor structure configurations are presented. In Figure 3, the SPR curves for four different designs applied to the prism are shown. With NK51A Prism, a single-layer configuration of silver (Ag) and nickel (Ni) is shown in Figure 3(a). This configuration results in a 2.65-degree change in the SPR angle and an angular sensitivity of 132.5 degrees/RIU. A modified configuration is shown in Figure 3(b) that contrast to traditional designs. A second layer of graphene (G) sits between the nickel and silver in this configuration. The SPR angle shifts by 2.70 degrees as a result of this configuration, and the obtained angular sensitivity is 135 degrees/RIU. A layer of KbNO3 is integrated on nickel in Figure 3(c). Increased angular sensitivity of 160 deg./RIU is obtained with this configuration, which results in an SPR angle variation of 3.20 deg. An additional layer in Figure 3(d) has also been shown to exhibit an SPR angle shift of 3.44 deg, attaining a larnge range of 1.330 to 1.350 for the reflective index. Also, other important parameters have also been calculated and results are shown in Table 2 for all four different SPR sensor configurations.

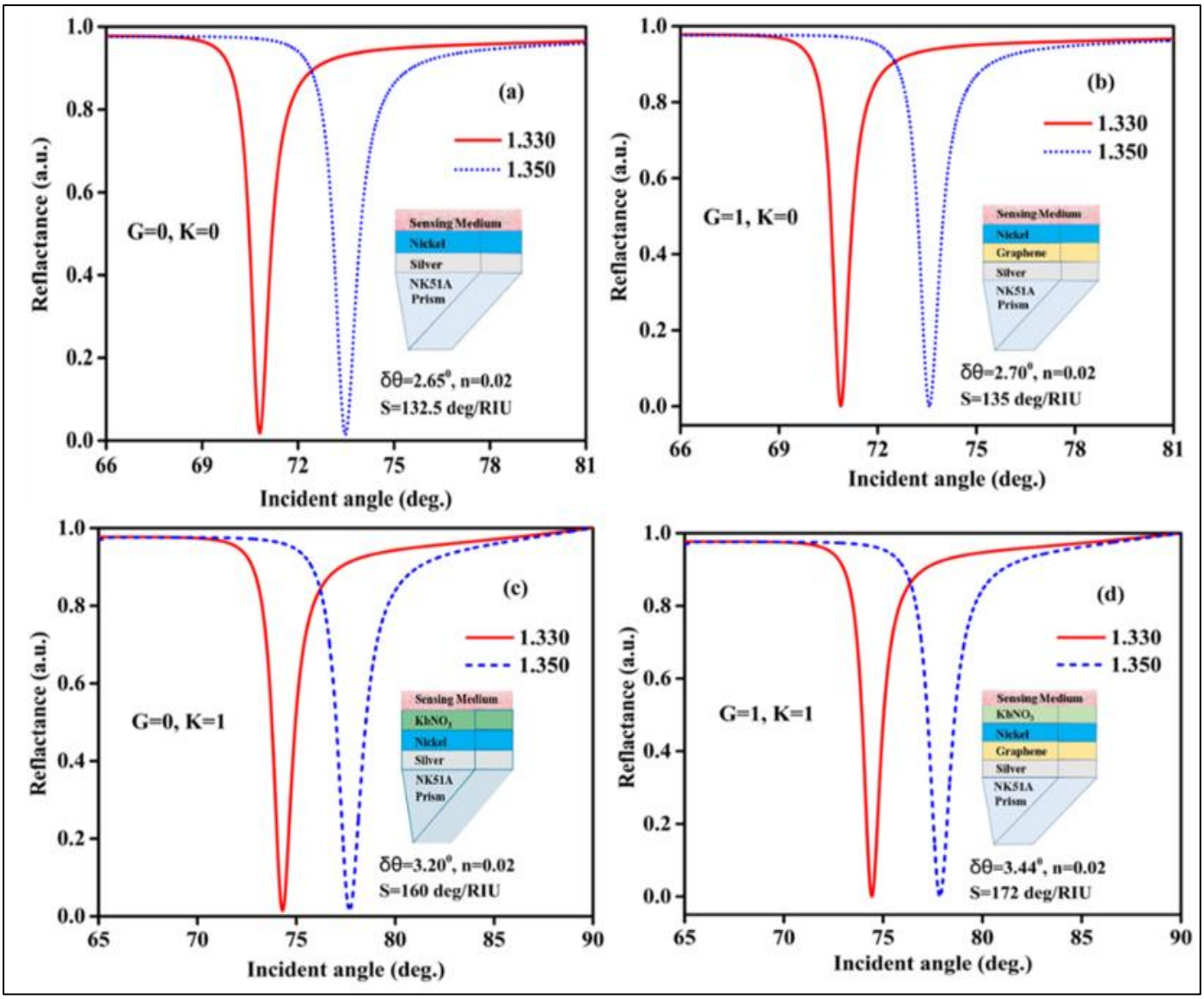

Fig 3 Different Configurations of Proposed SPR Sensor.

Table 2 Calculated Performance Paramrtrs for Various Layer Configurations Used in the SPR Biosensor Between RI 1.330-1.350 (δn=0.02).

Different Cases	Change in Resonance Angle (δθ)	Sensitivity (deg/RIU)	FWHM (deg)	Detection Accuracy (deg^{-1})	Figure of Merit (RIU^{-1})	Limit of dictation ($x10^{-6}$)
G=0, K=0	2.65	132.50	1.8882	0.529	70.482	7.547
G=1, K=0	2.70	135.00	1.8753	0.533	72.000	7.407
G=0, K=1	3.20	160.00	1.8332	0.545	87.283	6.250
G=1, K=1	3.44	172.00	1.8209	0.549	94.453	5.814

ISSN No: -2456-2165 https://doi.org/10.38124/ijisrt/25oct1379

➢ *Prism Selection and Metal Layer Thickness Optimization*

The angular behaviour of the Surface Plasmon Resonance (SPR) sensor plays a pivotal role in determining the most suitable material for the glass prism. Detailed experimental and theoretical analyses have demonstrated that utilizing a glass prism with a lower refractive index results in a more substantial alteration of the reflectance curve across broader angular ranges, thereby amplifying the angular sensitivity of the SPR sensor. This research employs an NFK51A glass prism, distinguished by its notably low refractive index, to expand the resonance angle over a wider angular range, thus enhancing angular responsiveness.

The visual data presented in Figure 4a illustrates the variation in the reflectance curve across different glass prisms, including NFK51A, BK7, SF10, and SF11. Among these, the NFK51A prism shows the most pronounced shift while preserving the lowest reflectance value (Rmin). Furthermore, Figure 4b highlights the fluctuations in angular sensitivity linked to variations in the refractive index of the glass prism integrated into our sophisticated SPR sensor design. The NFK51A prism, with its exceptionally low refractive index, proves instrumental in attaining peak angular sensitivity, making it the preferred option for optimizing the optical efficacy of the proposed SPR sensor system.

In addition to the choice of prism material, fine-tuning the thickness of the silver (Ag) metal layer is essential for achieving the minimal reflectance (R_{min}) at the resonance angle. Rmin, a critical optical metric, represents the smallest energy dissipation from the incident light to the surface plasmons formed at the metal-dielectric boundary. The precisely adjusted thickness of the Ag layer profoundly affects the intensity of the evanescent field and the overall sensitivity of the SPR sensor. At a thickness of 45 nm, the Ag layer exhibits optimal sensitivity alongside the lowest R_{min} value.

Figures 4c and 4d provide a graphical depiction of the changes in the reflectance curve and the sensitivity of the SPR sensor across various thicknesses of the Ag metal layer. The data clearly indicates that at a thickness of 45 nm, the angular sensitivity of the proposed SPR sensor reaches its highest level. Consequently, both the selection of the NFK51A glass prism and the optimization of the Ag layer thickness are critical factors in maximizing the performance of this advanced SPR sensor technology.

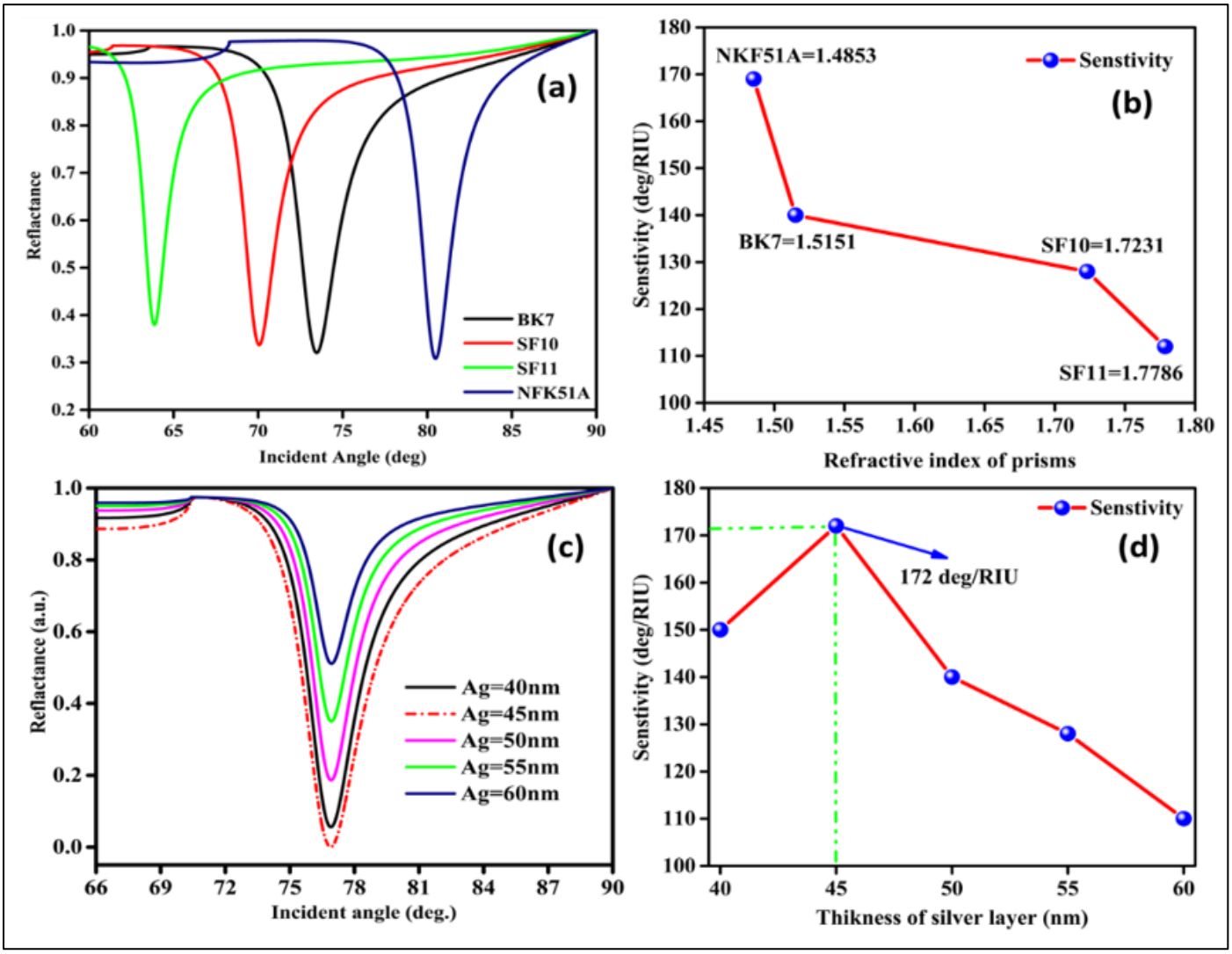

Fig 4 Prism Selection and Ag Metal Thikness Optimization Corresponding Angular Sensitivity.

ISSN No: -2456-2165 https://doi.org/10.38124/ijisrt/25oct1379

➢ *Effect of Graphene and $KbNO_3$ Layer*

The effect of incorporating $KbNO_3$ (K) and graphene (G) layers over the metal layer is depicted in Figure 5. The refractive index (RI) of the sensing medium is kept within the range of 1.330 to 1.350, and the associated angular sensitivity measurements are recorded in Table 2. The evaluation conducted reveals a distinct improvement in sensitivity upon the addition of single layers of both K and G over the standard SPR configuration, represented as K=0, G=0 (Prism + Metal). This improvement manifests as a rise in sensitivity from 132.5 deg./RIU to 172 deg./RIU, when K=0 and G =1 (indicating no K layer but the presence of a G layer). Moreover, with the inclusion of a single K layer and the absence of G (denoted as K=1, G=0), the sensitivity is significantly elevated to 160 deg./ RIU. Finally, in the suggested setup where both K=1 and G=1, the sensitivity peaks at 172 deg./RIU. Concerning the variation in the number of graphene layers while maintaining a constant $KbNO_3$ layer, it is evident that such changes influence the shape of the SPR curves. Specifically, an increase in the number of graphene layers causes the SPR curves to shift toward greater angles of incidence. A comparable trend is observed when altering the number of $KbNO_3$ layers, which impacts the width of the SPR curves. It should be noted that the refractive index (RI) remains fixed at 1.330-1.350 throughout these observations.

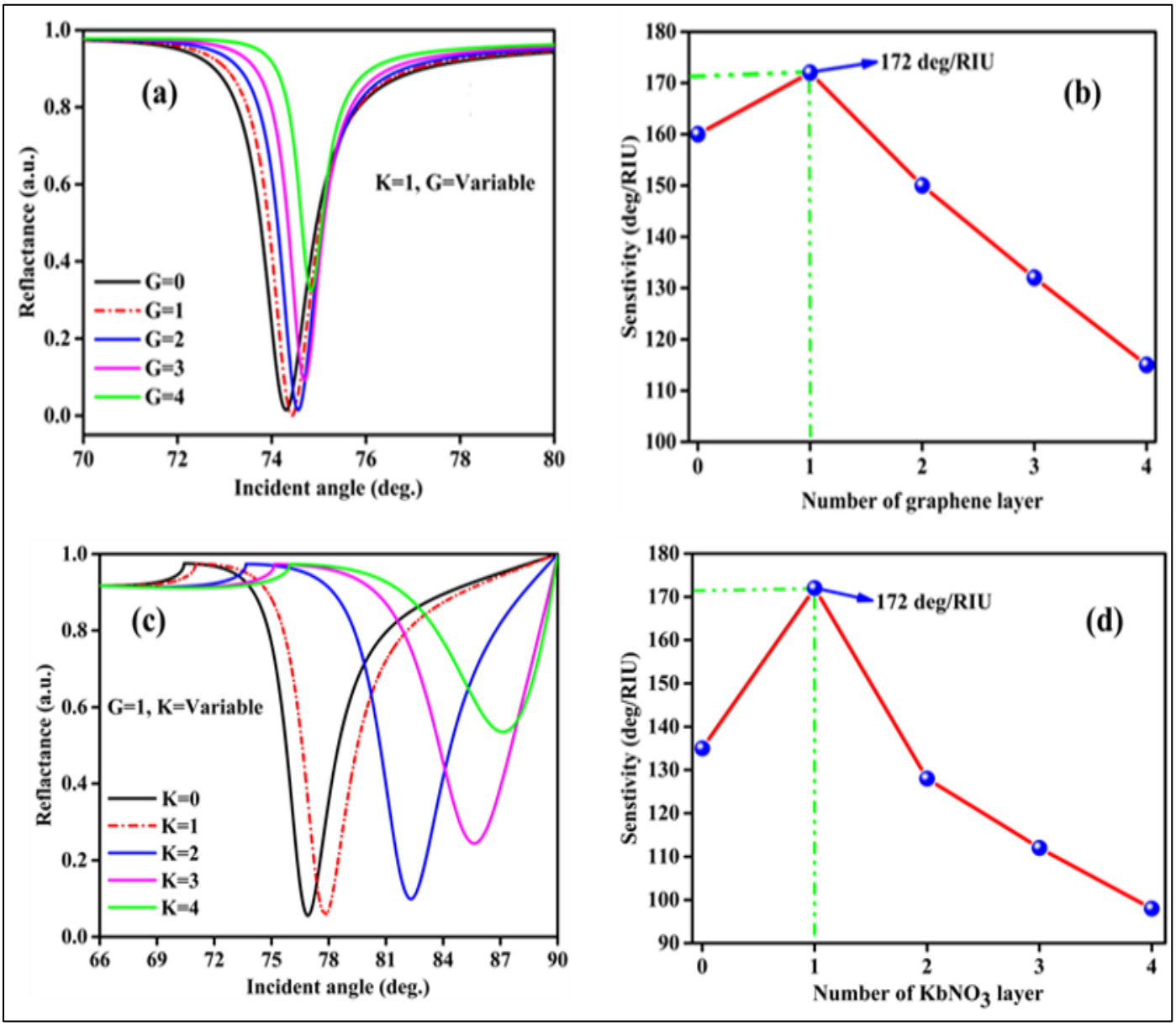

Fig 5 Thikness Optimization of Graphene and $KbNO_3$ Multilayers Corresponding Angular Sensitivity.

➢ *Electric Field Intensity and Penetration Depth Optimization*

Figure 6 illustrates how the electric field intensity distribution has been utilized to understand the performance parameters of the described SPR sensor. The offered SPR sensor enhancing the penetration depth and provides a powerful electro field intensity (17.28 V/m). Since, the electric field intensity at which the penetration depth decreases is proportional to (1/e) times. Thus the optimum penetration depth of proposed SPR sensor is 91.12 nm.

ISSN No: -2456-2165 https://doi.org/10.38124/ijisrt/25oct1379

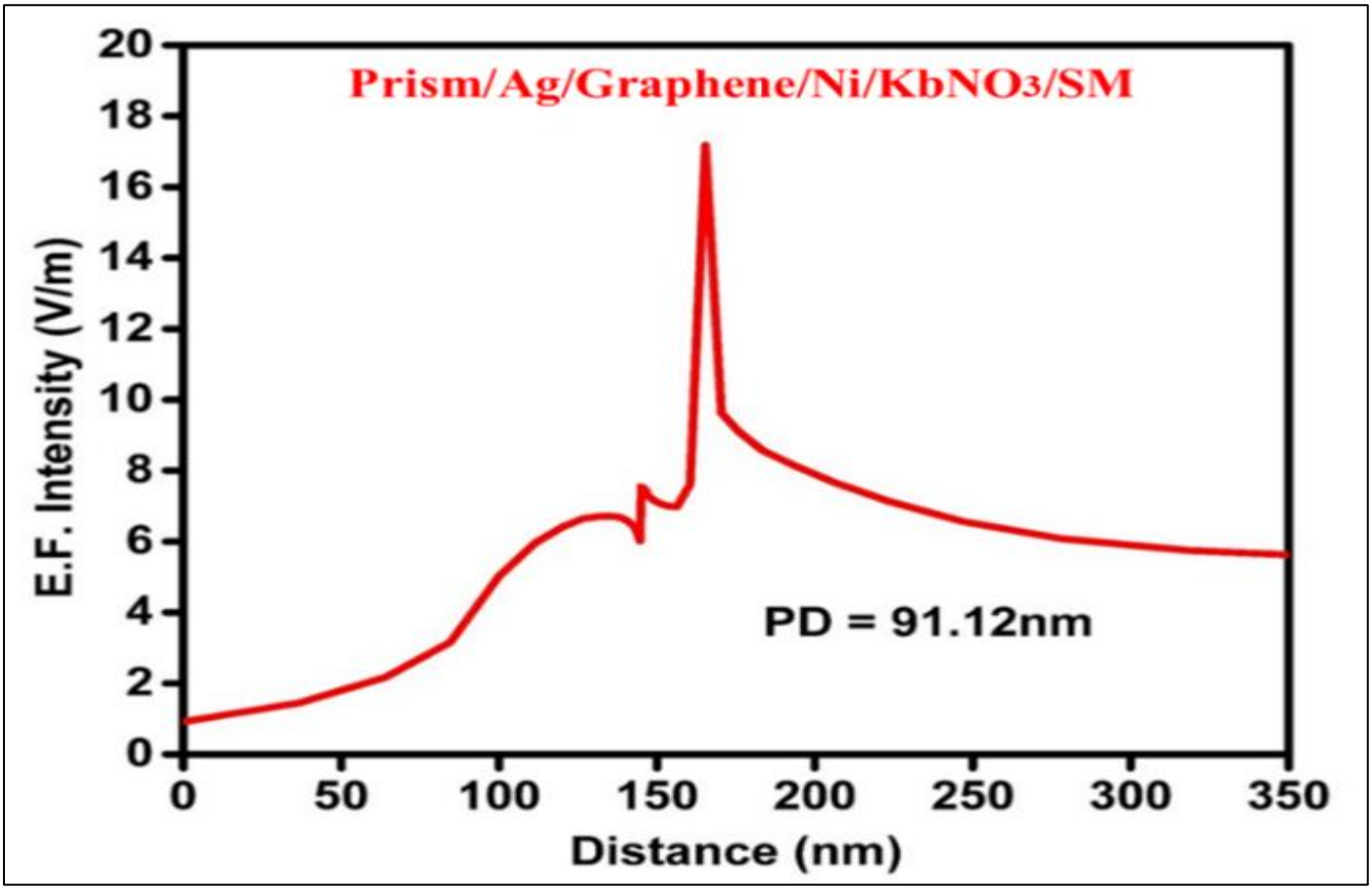

Fig 6 Optimized Electric Field and Penetration Depth of Proposed SPR Sensor.

Additionally, Table 3 illustrates that proposed SPR sensor significant efficiency among existing SPR-based designs in terms of angular sensitivity, detection ability and quality factor.

Table 3 An Analysis that Compares Some Recently Published SPR Sensor Works.

Layer Configuration	Sensitivity (deg/RIU)	QF (RIU^{-1})	DA (deg^{-1})	References
CaF_2/Au/$BaTiO_3$/WSe_2/SM	128.58	30.07	4.50	[52]
SF11/Au/MoS_2/Graphene/SM	130.00	47.02	1.37	[53]
BAK7/ZnO/Ag/$PtSe_2$/Graphene/SM	155.33	51.00	0.73	[54]
BK7/Ag/MXene/Ag/ZnO/Graphene/SM	161.00	67.93	0.64	[55]
NK51A/Ag/Graphene/Ni/$KbNO_3$/SM	172.00	94.45	0.55	Present Work

IV. CONCLUSION

The present investigation reports a theoretical study of a hybrid nanostructure of the SPR refractive index sensor (NK51A/Ag/Graphene/Ni/$KbNO_3$/SM). After the various layers of nanomaterials were deposited, the maximum angular sensitivity has been achieved. The stacking of many layers of nanomaterials in a decaying order of work function has improved the sensing performance by enhancing the flow of charge carriers towards the metal–dielectric interface and achieving surface plasmon resonance conditions. These materials contribute to improving the SPR sensor performance parameters because of their distinct optical, electrical, and physical characteristics. The anisotropic character of Nickel also improves the penetration depth in the sensing medium for various RI analytes and aids in fine-tuning the values of performance parameters. The described SPR sensor creates new possibilities for the development in the domain of biomedical, biochemical, and biological applications.

AKNOWLEDGEMENT

➢ *Credit Authorship & Contribution Statement*

Shalini Srivastava: Conceptualization, Software, & Writing Original Draft Preparation. Ramesh Mishra & Parimal Tiwari: Visualization & Research Validation, Shambhavi Mudra Shukla & Nishant Singh: Supervision & Reviewing: Sachin Singh, Mukesh Mishra & Vaibhava Srivastava: Editing & Validating. Vipin Sharma: Revising manuscript.

- Corresponding Author: Sachin Singh.
- Funding: There is no funding offered for this article.
- Data Availability: During the current study, no datasets were created or examined.

ISSN No: -2456-2165 https://doi.org/10.38124/ijisrt/25oct1379

- Declaration
- Competing Interest: On behalf of all authors, the corresponding author states that there is no conflict of interest.
- Ethical Approval: Not applicable.

REFERENCES

[1]. Buk Cardoso, L., Cunha Parro, V., Verzinhasse Peres, S., Curado, M. P., Fernandes, G. A., Wünsch Filho, V., & Natasha Toporcov, T. (2023). Machine learning for predicting survival of colorectal cancer patients. Scientific reports, 13(1), 8874.

[2]. Schinkel, M., Bennis, F. C., Boerman, A. W., Wiersinga, W. J., & Nanayakkara, P. W. (2023). Embracing cohort heterogeneity in clinical machine learning development: a step toward generalizable models. Scientific reports, 13(1), 8363.

[3]. Koh, D. M., Papanikolaou, N., Bick, U., Illing, R., Kahn Jr, C. E., Kalpathi-Cramer, J., ... & Prior, F. (2022). Artificial intelligence and machine learning in cancer imaging. Communications Medicine, 2(1), 133.

[4]. Lambert, S. I., Madi, M., Sopka, S., Lenes, A., Stange, H., Buszello, C. P., & Stephan, A. (2023). An integrative review on the acceptance of artificial intelligence among healthcare professionals in hospitals. NPJ Digital Medicine, 6(1), 111.

[5]. Zador, A., Escola, S., Richards, B., Ölveczky, B., Bengio, Y., Boahen, K., ... & Tsao, D. (2023). Catalyzing next-generation artificial intelligence through neuroai. Nature communications, 14(1), 1597.

[6]. Chen, Y. C. (2022). The Need for a System View to Regulate Artificial Intelligence/Machine Learning-Based Software as Medical Device. Angle Health Law Review, (64), 111-125.

[7]. Sun, Y. K., Zhou, B. Y., Miao, Y., Shi, Y. L., Xu, S. H., Wu, D. M., ... & Xu, H. X. (2023). Three-dimensional convolutional neural network model to identify clinically significant prostate cancer in transrectal ultrasound videos: a prospective, multi-institutional, diagnostic study. EClinicalMedicine, 60.

[8]. Homma, Y., Ito, S., Zhuang, X., Baba, T., Fujibayashi, K., Kaneko, K., & Ishijima, M. (2022). Artificial intelligence for distinguishment of hammering sound in total hip arthroplasty. Scientific Reports, 12(1), 9826.

[9]. Stafford, I. S., Kellermann, M., Mossotto, E., Beattie, R. M., MacArthur, B. D., & Ennis, S. (2020). A systematic review of the applications of artificial intelligence and machine learning in autoimmune diseases. NPJ digital medicine, 3(1), 30.

[10]. Fu, T., Zang, Y., Huang, Y., Du, Z., Huang, H., Hu, C., ... & Chen, H. (2023). Photonic machine learning with on-chip diffractive optics. Nature Communications, 14(1), 70.

[11]. Khodaie, A. and Heidarzadeh, H., 2025. Ultra-sensitive surface plasmon resonance sensor integrating MXene (Ti3C2TX) and graphene for advanced carcinoembryonic antigen detection. Scientific Reports, 15(1), p.13571.

[12]. Khodaie, A., Javidan, J. and Heidarzadeh, H., 2025. Development of a Surface Plasmon Resonance Sensor using 2D Materials, Including Graphene and Black Phosphorus, for Measuring Water Pressure. Plasmonics, pp.1-12.

[13]. Peurifoy, J., Shen, Y., Jing, L., Yang, Y., Cano-Renteria, F., DeLacy, B. G., & Soljačić, M. (2018). Nanophotonic particle simulation and inverse design using artificial neural networks. Science advances, 4(6), eaar4206.

[14]. Rivenson, Y., Göröcs, Z., Günaydin, H., Zhang, Y., Wang, H., & Ozcan, A. (2017). Deep learning microscopy. Optica, 4(11), 1437-1443.

[15]. Carleo, G., & Troyer, M. (2017). Solving the quantum many-body problem with artificial neural networks. Science, 355(6325), 602-606.

[16]. Lin, X., Rivenson, Y., Yardimci, N. T., Veli, M., Luo, Y., Jarrahi, M., & Ozcan, A. (2018). All-optical machine learning using diffractive deep neural networks. Science, 361(6406), 1004-1008.

[17]. Khodaie, A. and Heidarzadeh, H., 2025. Enhanced Surface Plasmon Resonance Biosensor for Carcinoembryonic Antigen Detection Using 2D Materials (Graphene and MoS2) in a Kretschmann Configuration. Plasmonics, pp.1-12.

[18]. Khodaie, A., Bahador, H. and Heidarzadeh, H., 2025. Development of a Surface Plasmon Resonance Sensor Based MXene (Ti 3 C 2 T x) for the Detection of Carcinoembryonic Antigen (CEA). Plasmonics.

[19]. Singh S, Singh PK, Umar A, Lohia P, Albargi H, Castañeda L, Dwivedi DK. 2D Nanomaterial-Based Surface Plasmon Resonance Sensors for Biosensing Applications. Micromachines. 2020; 11(8):779.

[20]. Singh, S., Sharma, A.K., Lohia, P. and Dwivedi, D.K., 2021. Theoretical analysis of sensitivity enhancement of surface plasmon resonance biosensor with zinc oxide and blue phosphorus/MoS2 heterostructure. Optik, 244, p.167618.

[21]. Ren, H. (2019, June). Three-dimensional Vectorial Holography. In The European Conference on Lasers and Electro-Optics (p. ck_7_5). Optica Publishing Group.

[22]. Sun, W., Kalmady, S. V., Sepehrvand, N., Salimi, A., Nademi, Y., Bainey, K., ... & Kaul, P. (2023). Towards artificial intelligence-based learning health system for population-level mortality prediction using electrocardiograms. NPJ Digital Medicine, 6(1), 21.

[23]. Meskó, B., & Görög, M. (2020). A short guide for medical professionals in the era of artificial intelligence. NPJ digital medicine, 3(1), 126.

[24]. Loftus, T. J., Shickel, B., Ozrazgat-Baslanti, T., Ren, Y., Glicksberg, B. S., Cao, J., ... & Bihorac, A. (2022). Artificial intelligence-enabled decision support in nephrology. Nature Reviews Nephrology, 18(7), 452-465.

[25]. Zhang, X., Song, X., Li, W., Chen, C., Wusiman, M., Zhang, L., & Lv, X. (2023). Rapid diagnosis of membranous nephropathy based on serum and urine Raman spectroscopy combined with deep learning methods. Scientific Reports, 13(1), 3418.

ISSN No: -2456-2165 https://doi.org/10.38124/ijisrt/25oct1379

[26]. Siontis, K. C., Noseworthy, P. A., Attia, Z. I., & Friedman, P. A. (2021). Artificial intelligence-enhanced electrocardiography in cardiovascular disease management. Nature Reviews Cardiology, 18(7), 465-478.
[27]. Saboe, D., Ghasemi, H., Gao, M.M., Samardzic, M., Hristovski, K.D., Boscovic, D., Burge, S.R., Burge, R.G. and Hoffman, D.A., 2021. Real-time monitoring and prediction of water quality parameters and algae concentrations using microbial potentiometric sensor signals and machine learning tools. Science of the Total Environment, 764, p.142876.
[28]. Gamal, H., Elkatatny, S. and Al Gharbi, S., 2023, October. Rig Sensor Data for AI-ML Technology-Based Solutions: Research, Development, and Innovations. In Abu Dhabi International Petroleum Exhibition and Conference (p. D021S074R006). SPE.
[29]. Yarkan, S., 2025. A Novel Acoustic Source Localization Technique for Edge AI Applications: A Lightweight Framework and Implementation for IoT and Smart Sensing Devices. ELECTRICA, 25(1), pp.1-9.
[30]. Nomura, A. (2023). Digital health, digital medicine, and digital therapeutics in cardiology: current evidence and future perspective in Japan. Hypertension Research, 46(9), 2126-2134.
[31]. Scheetz, J., Rothschild, P., McGuinness, X., Soyer, H. P., Janda, M., ... & van Wijngaarden, P. (2021). A survey of clinicians on the use of artificial intelligence in ophthalmology, dermatology, radiology and radiation oncology. Scientific reports, 11(1), 5193.
[32]. Long, E., Chen, J., Wu, X., Liu, Z., Wang, L., Jiang, J., ... & Liu, Y. (2020). Artificial intelligence manages congenital cataract with individualized prediction and telehealth computing. NPJ digital medicine, 3(1), 112.
[33]. Ciecierski-Holmes, T., Singh, R., Axt, M., Brenner, S., & Barteit, S. (2022). Artificial intelligence for strengthening healthcare systems in low-and middle-income countries: a systematic scoping review. NPJ digital medicine, 5(1), 162.
[34]. Tagliaferri, S. D., Angelova, M., Zhao, X., Owen, P. J., Miller, C. T., Wilkin, T., & Belavy, D. L. (2020). Artificial intelligence to improve back pain outcomes and lessons learnt from clinical classification approaches: three systematic reviews. NPJ digital medicine, 3(1), 93.
[35]. Sermesant, M., Delingette, H., Cochet, H., & Ayache, N. (2021). Applications of artificial intelligence in cardiovascular imaging. Nature Reviews Cardiology, 18(8), 600-609.
[36]. Yu, K. H., Beam, A. L., & Kohane, I. S. (2018). Artificial intelligence in healthcare. Nature biomedical engineering, 2(10), 719-731.
[37]. Song, X., Yu, A. S., Kellum, J. A., Waitman, L. R., Matheny, M. E., Simpson, S. Q., ... & Liu, M. (2020). Cross-site transportability of an explainable artificial intelligence model for acute kidney injury prediction. Nature communications, 11(1), 5668.
[38]. Gao, X., Zhang, Z. Y., & Duan, L. M. (2018). A quantum machine learning algorithm based on generative models. Science advances, 4(12), eaat9004.
[39]. Orzechowski, P., & Moore, J. H. (2022). Generative and reproducible benchmarks for comprehensive evaluation of machine learning classifiers. Science Advances, 8(47), eabl4747.
[40]. Fanconi, C., De Hond, A., Peterson, D., Capodici, A., & Hernandez-Boussard, T. (2023). A Bayesian approach to predictive uncertainty in chemotherapy patients at risk of acute care utilization. EBioMedicine, 92.
[41]. Hamadani, A., Ganai, N. A., Mudasir, S., Shanaz, S., Alam, S., & Hussain, I. (2022). Comparison of artificial intelligence algorithms and their ranking for the prediction of genetic merit in sheep. Scientific Reports, 12(1), 18726.
[42]. Jia, Z., Chen, J., Xu, X., Kheir, J., Hu, J., Xiao, H., ... & Shi, Y. (2023). The importance of resource awareness in artificial intelligence for healthcare. Nature Machine Intelligence, 5(7), 687-698.
[43]. Mondal, H. S., Ahmed, K. A., Birbilis, N., & Hossain, M. Z. (2023). Machine learning for detecting DNA attachment on SPR biosensor. Scientific Reports, 13(1), 3742.
[44]. Rostov, M., Hossain, M. Z., & Rahman, J. S. (2021, August). Robotic emotion monitoring for mental health applications: Preliminary outcomes of a survey. In IFIP Conference on Human-Computer Interaction (pp. 481-485). Cham: Springer International Publishing.
[45]. Qin, A., Hasan, M. R., Ahmed, K. A., & Hossain, M. Z. (2022, June). Machine learning for predicting cancer severity. In 2022 IEEE 10th International Conference on Healthcare Informatics (ICHI) (pp. 527-529). IEEE.
[46]. Daskalaki, E., Parkinson, A., Brew-Sam, N., Hossain, M. Z., O'Neal, D., Nolan, C. J., & Suominen, H. (2022). The potential of current noninvasive wearable technology for the monitoring of physiological signals in the management of type 1 diabetes: literature survey. Journal of medical Internet research, 24(4), e28901.
[47]. Deng, J., Hasan, M. R., Mahmud, M., Hasan, M. M., Ahmed, K. A., & Hossain, M. Z. (2022, October). Diagnosing autism spectrum disorder using ensemble 3D-CNN: A preliminary study. In 2022 IEEE international conference on image processing (ICIP) (pp. 3480-3484). IEEE.
[48]. Bezzan, V. P., & Rocco, C.D (2021). Predicting special care during the COVID-19 pandemic: A machine learning approach. Health Information Science & Systems, 9(1), 34.
[49]. Hossain, M. Z., Daskalaki, E., Brüstle, A., Desborough, J., Lueck, C. J., & Suominen, H. (2022). The role of machine learning in developing non-magnetic resonance imaging based biomarkers for multiple sclerosis: a systematic review. BMC Medical Informatics and Decision Making, 22(1), 242.
[50]. Sharma, V., Dwivedi, L. K., Singh, S., Uniyal, A., Srivastava, V., & Singh, S. P. (2025). Analytical Study on Effect of Perovskite Halides based Surface Plasmon Resonance Sensor for Detection of Sugar Content in Soft Drinks. Sensing and Imaging, 26(1), 65.

ISSN No: -2456-2165 https://doi.org/10.38124/ijisrt/25oct1379

[51]. Srivastava, S., Yadav, S., Mishra, A. C., Singh, S., Lohia, P., Dwivedi, D. K., ... & Hossain, M. K. (2024). Ultra-sensitive surface plasmon resonance biosensor for liver metastases and hepatocellular carcinoma detection using silicon nitride and black phosphorus nanomaterial. Plasmonics, 19(2), 1031-1041.

[52]. Basak, C., Islam, M.S., Hosain, M.K. and Kouzani, A.Z., 2024. An ultra-sensitive surface plasmon resonance biosensor with PtSe2 and BlueP/WS2 heterostructure. Heliyon, 10(19).

[53]. Basak, C., Hosain, M.K., Islam, M.S. and Kouzani, A.Z., 2023. Design and modeling of an angular interrogation based surface plasmon resonance biosensor for dengue virus detection. Optical and Quantum Electronics, 55(5), p.438.

[54]. Kotha, V.V., Vankayalapati, S., Vasimalla, Y., Vaadaala, J., Jain, S., Ramachandran, B., Santhosh, C., Maloji, S. and Kumar, S., 2025. Ultra-sensitive prism-based surface plasmon resonance biosensor utilizing lead molybdate and BlueP/TDMC nanocomposites for early malaria detection. Plasmonics, 20(7), pp.5287-5302.

[55]. Karki, B., Vasudevan, B., Uniyal, A., Pal, A. and Srivastava, V., 2022. Hemoglobin detection in blood samples using a graphene-based surface plasmon resonance biosensor. Optik, 270, p.169947.